Shinya Aoi · Naomichi Ogihara · Tetsuro Funato ·
Yasuhiro Sugimoto · Kazuo Tsuchiya

Evaluating functional roles of phase resetting in generation of adaptive human bipedal walking with a physiologically-based model of the spinal pattern generator

Abstract The central pattern generators (CPGs) in the spinal cord strongly contribute to locomotor behavior. To achieve adaptive locomotion, locomotor rhythm generated by the CPGs is suggested to be functionally modulated by phase resetting based on sensory afferent or perturbations. Although phase resetting has been investigated during fictive locomotion in cats, its functional roles in actual locomotion have not been clarified. Recently, simulation studies have been conducted to examine the roles of phase resetting during human bipedal walking, assuming that locomotion is generated based

S. Aoi
Dept. of Aeronautics and Astronautics, Graduate School of Engineering, Kyoto University, Yoshida-honmachi, Sakyo-ku, Kyoto 606-8501, Japan
E-mail: shinya_aoi@kuaero.kyoto-u.ac.jp

N. Ogihara
Dept. of Mechanical Engineering, Faculty of Science and Technology, Keio University, 3-14-1 Hiyoshi, Kohoku-ku, Yokohama 223-8522, Japan

T. Funato
Dept. of Mechanical Engineering and Science, Graduate School of Engineering, Kyoto University, Yoshida-honmachi, Sakyo-ku, Kyoto 606-8501, Japan

Y. Sugimoto
Dept. of Mechanical Engineering, Graduate School of Engineering, Osaka University, Yamadaoka 2-1, Suita, Osaka 565-0871, Japan

K. Tsuchiya
Dept. of Energy and Mechanical Engineering, Faculty of Science and Engineering, Doshisha University, 1-3 Tatara, Miyakodani, Kyotanabe, Kyoto 610-0394, Japan

S. Aoi and K. Tsuchiya
JST, CREST, 5 Sanbancho, Chiyoda-ku, Tokyo 102-0075, Japan

on prescribed kinematics and feedback control. However, such kinematically-based modeling cannot be used to fully elucidate the mechanisms of adaptation. In this paper, we proposed a more physiologically-based mathematical model of the neural system for locomotion and investigated the functional roles of phase resetting. We constructed a locomotor CPG model based on a two-layered hierarchical network model of the rhythm generator (RG) and pattern formation (PF) networks. The RG model produces rhythm information using phase oscillators and regulates it by phase resetting based on foot-contact information. The PF model creates feedforward command signals based on rhythm information, which consists of the combination of five rectangular pulses based on previous analyses of muscle synergy. Simulation results showed that our model establishes adaptive walking against perturbing forces and variations in the environment, with phase resetting playing important roles in increasing the robustness of responses, suggesting that this mechanism of regulation may contribute to the generation of adaptive human bipedal locomotion.

1 Introduction

Physiological studies suggest that the central pattern generators (CPGs) in the spinal cord strongly contribute to rhythmic limb movement, such as locomotion (Grillner 1975; Orlovsky *et al.* 1999; Shik and Orlovsky 1976). The CPGs can produce oscillatory behaviors even in the absence of rhythmic input and proprioceptive feedback. However, they must use sensory feedback to produce effective locomotor behavior. Experimental studies have shown that sensory feedback modulates locomotor rhythm and its phase so as to reset the locomotor rhythm induced by a shift in the phase based on sensory afferents and perturbations (phase resetting), as observed in electromyographic (EMG) and electroneurographic (ENG) examinations of cats (Conway *et al.* 1987; Duysens 1977a; Guertin *et al.* 1995; Lafreniere-Roula and McCrea 2005; Schomburg *et al.* 1998). Although these findings have been accumulated based on animal experiments, there is also clinical evidence suggesting that such CPGs also exist in the human spinal cord (Hultborn and Nielsen 2007; Minassian *et al.* 2007).

Since the rhythm and phase modulations in phase resetting have for the most part been investigated during fictive locomotion, their functional roles during actual locomotion remain largely unclear. To overcome this limitation, simulation studies have recently been performed, the physiological and anatomical findings of which allow the construction of reasonably realistic mathematical models of the musculoskeletal and nervous systems and investigation of specific functional roles in locomotor behavior (Ekeberg and Pearson 2005; Frigon and Rossignol 2006; Ijspeert 2001; Taga *et al.* 1991;

Taga 1995a; Taga 1995b; Wadden and Ekeberg 1998; Yakovenko *et al.* 2004). To examine the functional roles of phase resetting during human bipedal locomotion, Yamasaki *et al.* (2003a, 2003b), Nomura *et al.* (2009), and Aoi *et al.* (2008) determined joint angles from measured kinematic data during human bipedal walking and examined mechanisms of adaptation to perturbing forces, with direct modulation of joint motions by incorporating phase resetting mechanisms. Their simulations demonstrated that sensory regulation improves the robustness of responses during human bipedal locomotion.

However, since these simulations assumed that locomotion is generated based on prescribed kinematics and feedback control, they are unable to reproduce various situation-dependent patterns of gait, and the adaptability they yield is limited. In addition, feedback control in joint kinematics easily destabilizes movements due to delay in signal transmission; this issue is of crucial importance. Such kinematically-based modeling has limitations in fully elucidating mechanisms of adaptation. Ivanenko *et al.* (2004, 2006) noted that although EMG data recorded during human bipedal locomotion are complex, they can be accounted for by the combination of only five basic patterns, suggesting that the CPGs produce such basic patterns and that α-motoneurons receive inputs representing combinations of these basic patterns through interneurons. This can be explained by feedforward signal generation in CPG function, and suggests that adequate modeling of feedforward control mechanisms in CPGs is crucial to investigation of mechanisms of adaptation in locomotor behavior.

In this paper, we propose a more physiologically-based mathematical model of the neural system for locomotion, and investigate the functional roles of phase resetting. The organization of CPGs remains unclear and various CPG models, such as the half-center model and the unit burst generator model, have been proposed (Guertin 2009; McCrea and Rybak 2008). However, recent neurophysiological findings suggest that CPGs consist of hierarchical networks, including rhythm generator (RG) and pattern formation (PF) networks (Burke *et al.* 2001; Lafreniere-Roula and McCrea 2005; Rybak *et al.* 2006a; Rybak *et al.* 2006b). The RG network generates the basic rhythm and alters it by producing phase shift and rhythm resetting based on sensory afferents and perturbations. The PF network shapes the rhythm into spatiotemporal patterns of activation of motoneurons through interneurons. In the present study, a locomotor CPG model was constructed based on the two-layered hierarchical network model. In this model, the RG network produces rhythm information using phase oscillators and regulates it by phase resetting based on foot-contact information. Furthermore, the PF model creates feedforward command signals based on rhythm information composed of combinations of five rectangular pulses. Simulation results showed that our model establishes adaptive walking against perturbing forces and variations in the environment despite the inclusion of substantial time delays attributed to neural transmission, with phase resetting playing important roles in increasing the robustness of responses,

suggesting that this mechanism of regulation may contribute to the generation of adaptive human bipedal locomotion.

This paper is organized as follows: Section 2 introduces our neuromusculoskeletal model, Section 3 presents results of simulations performed to investigate the mechanisms of adaptation involving phase resetting against perturbing forces and environmental variations, and Section 4 is a discussion and presentation of conclusions.

2 Model

2.1 Skeletal model

We used seven rigid links for the skeletal model that represent the HAT (head, arms, and trunk), thighs, shanks, and feet (Fig. 1**A**). The physical parameters used in this study are described in Aoi *et al.* (2008) and Ogihara and Yamazaki (2001) and were determined using the regression equations in Winter (2004). Each joint is modeled as a pin joint. The joint angles are zero when this model stands straight, with the trunk, thigh, and shank in a straight line and perpendicular to the sole of the foot. When a link rotates in an anticlockwise direction relative to the proximal link, the joint angle increases. Each joint has a linear viscous element, and the coefficients of viscosity for the hip, knee, and ankle joints are 1.09, 3.17, and 0.943 Nms/rad, respectively (Davy and Audu 1987). The angles of the knee and ankle joints have limited ranges of motion, from -2.8 to -0.1 rad and -1.0 to 0.54 rad, respectively. When these joint angles exceed their limits, they are subject to large linear elastic and damping torque. The elastic and viscous coefficients are 2.0×10^3 Nm/rad and 3.0×10^2 Nms/rad for the knee joint and 2.0×10^2 Nm/rad and 30 Nms/rad for the ankle joint.

When the foot makes contact with the ground, it receives a reaction force from the ground. We employed four contact points on the sole to receive this force: toe, heel, and 4.0 cm inside from the toe and from the heel. The reaction force is modeled by a linear spring and damper system. The coefficients of elasticity and viscosity are 5.0×10^3 N/m and 1.0×10^2 Ns/m horizontally and 2.5×10^4 N/m and 5.0×10^2 Ns/m vertically. We derived the equation of motion using Lagrangian equations and solved the equation of motion using the fourth-order Runge-Kutta method with time steps of 0.1 ms for numerical simulation.

2.2 Muscle model

For the muscle model (Fig. 1**B**), we used nine principal muscles for each leg; six muscles are uniarticular: hip flexion (Iliopsoas (IL)), hip extension (Gluteus Maximus (GM)), knee extension (Vastus (VA)),
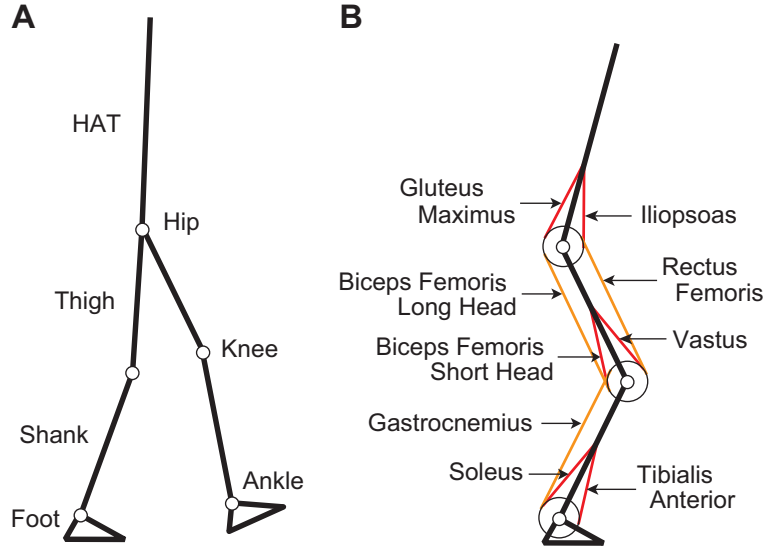
Fig. 1 Musculoskeletal model (Aoi *et al.* 2008; Ogihara and Yamazaki 2001). **A** shows the skeletal model composed of seven rigid links that represent HAT (head, arms, and trunk), thighs, shanks, and feet. **B** shows the muscle model for one leg composed of nine principal muscles; six muscles (IL, GM, VA, BFS, TA, and SO) are uniarticular and three (RF, BFL, and GC) are biarticular.

knee flexion (Biceps Femoris Short Head (BFS)), ankle flexion (Tibialis Anterior (TA)), and ankle extension (Soleus (SO)), and three muscles are biarticular: hip flexion and knee extension (Rectus Femoris (RF)), hip extension and knee flexion (Biceps Femoris Long Head (BFL)), and knee flexion and ankle extension (Gastrocnemius (GC)). The moment arms of the muscles around the joints are constant, regardless of joint angles. When the joints are at their neutral angles, the muscles are at their optimal lengths. The neutral angles are 0.0, -0.52, and 0.0 rad for the hip, knee, and ankle joints, respectively (Aoi *et al.* 2008; Ogihara and Yamazaki 2001).

A muscle receives a signal from the corresponding α-motoneuron and generates muscle tension depending on the force-length and force-velocity relationships. We used the mathematical model in Aoi *et al.* (2008) and Ogihara and Yamazaki (2001), composed of a contractile element (CE) and passive elastic (PE) and damping (PD) elements parallel to CE, as follows:

$$F_m = \bar{F}_m^{CE} \cdot k(\xi_m) \cdot h(\eta_m) \cdot a_m + F_m^{PD} + F_m^{PE}$$

$$k(\xi_m) = 0.32 + 0.71 \exp[-1.112(\xi_m - 1)] \sin[3.722(\xi_m - 0.656)]$$

$$h(\eta_m) = 1 + \tanh(3.0\eta_m) \tag{1}$$

$$F_m^{PD} = c_m^{PD} \dot{L}_m$$

$$F_m^{PE} = k_m^{PE}\{\exp[15(L_m - \bar{L}_m)] - 1\}$$

where F_m (m = IL, GM, VA, BFS, TA, SO, RF, BFL, and GC) is the muscle tension, $\bar{F}_m^{CE}$ is the maximum muscle tension produced by CE, $k(\xi_m)$ is the force-length relationship, $h(\eta_m)$ is the force-velocity relationship, ξ_m and η_m are the normalized muscle length and contractile velocity divided by the muscle optimal length and maximum muscle contractile velocity, a_m is the muscle activation ($0 \leq a_m \leq 1$), F_m^{PD} and F_m^{PE} are the forces generated by the damping and elastic elements, c_m^{PD} is the viscous coefficient, and k_m^{PE} is the coefficient of the elastic element. These parameters are used in Aoi *et al.* (2008) and Ogihara and Yamazaki (2001), and were determined based on anatomical charts and proposed models in Davy and Audu (1987). Note that although the force-length relationship $k(\xi_m)$ is negative when the normalized muscle length ξ_m is less than 0.58, the normalized muscle length is never that short during locomotion.

Muscle activation a_m determines the muscle tension generated by the contractile element of the muscle, the dynamics of which are given by a low-pass filter (Fuglevand and Winter 1993; Jo and Massaquoi 2007; Jo 2008)

$$LF_m(s) = \frac{\rho^2}{(s+\rho)^2}$$
$$a_m = LF_m(s)(u_m) \tag{2}$$

where $\rho = 30$ rad/s and u_m is the output from the α-motoneuron determined by the model of the nervous system.

2.3 Nervous system model

The α-motoneuron receives command signals produced through a neural network and information processing in the motor cortex, brainstem, cerebellum, and spinal cord. For simplicity, we assume that the output u_m from the α-motoneuron is the result of the following three components:

1. Movement control, which produces periodic signals in feedforward fashion at the spinal cord level to create periodic limb movements for forward motion;
2. Phase resetting, which modulates timing to produce the feedforward signals of the movement controller at the spinal cord level based on sensory signals; and
3. Posture control, which creates command signals in feedback fashion based on somatosensory information at the brainstem and cerebellar levels to control and regulate postural behavior.

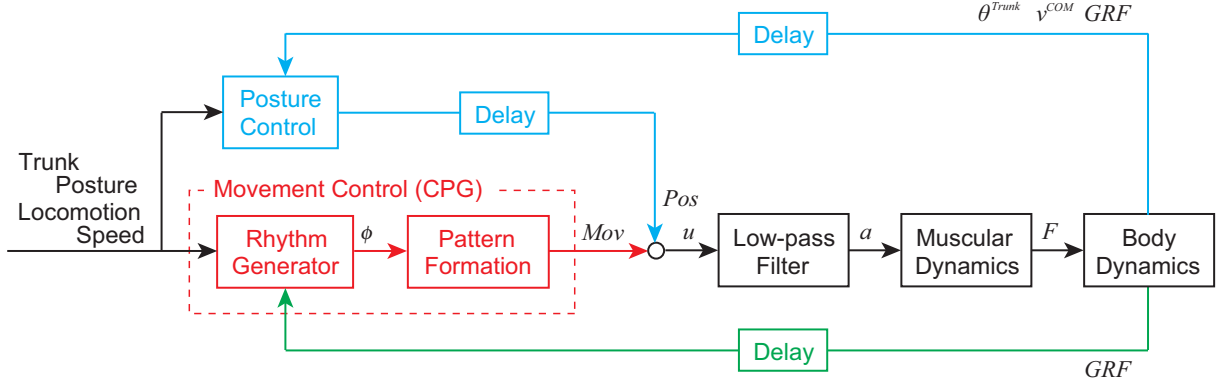Therefore, output u_m is given by

$$u_m = Mov_m + Pos_m \tag{3}$$

Fig. 2 Nervous system model. Red blocks and arrows indicate movement control, blue blocks and arrows indicate posture control, and green blocks and arrows indicate phase resetting.

where Mov_m and Pos_m are the outputs of the movement and posture controls, respectively. Figure 2 shows our model of the nervous system.

2.3.1 Movement control

Neurophysiological studies have suggested the important concept of muscle synergy in control of movement in humans and animals (d'Avella and Bizzi 2005; d'Avella *et al.* 2003; Drew *et al.* 2008; Danna-dos-Santos *et al.* 2007; Ivanenko *et al.* 2005; Ting and Macpherson 2005; Todorov and Jordan 2002), which has been examined using principal component analysis (PCA) and factor analysis (FA) and viewed as one means of coping with redundancy by decreasing the number of degrees of freedom. Muscle synergy is related to co-variation of muscle activity. As noted above, Ivanenko *et al.* (2004, 2006) reported that although the EMG data recorded during human bipedal locomotion are complex, they can be accounted for by the combination of only five basic patterns, as determined by PCA. They suggested that the CPGs produce the basic patterns and manage timing based on kinematic events, such as foot contact and foot off. The basic patterns are delivered to the α-motoneurons through interneurons, and the α-motoneuron receives combinations of the basic patterns (Fig. 3). Jo and Massaquoi (2007) and Jo (2008) prepared such basic patterns using rectangular pulses for the feedforward signals in their simulation model.

The organization of CPGs remains unclear and various CPG organizations have been proposed as described in the Introduction. Recently, neurophysiological findings suggest that the CPGs consist of hierarchical networks, including RG and PF networks (Burke *et al.* 2001; Lafreniere-Roula and McCrea 2005; Rybak *et al.* 2006a; Rybak *et al.* 2006b). The RG network generates the basic rhythm and alters it by producing phase shift and rhythm resetting based on sensory afferents and perturbations (phase resetting). The PF network shapes the rhythm into spatiotemporal patterns of activation of motoneurons
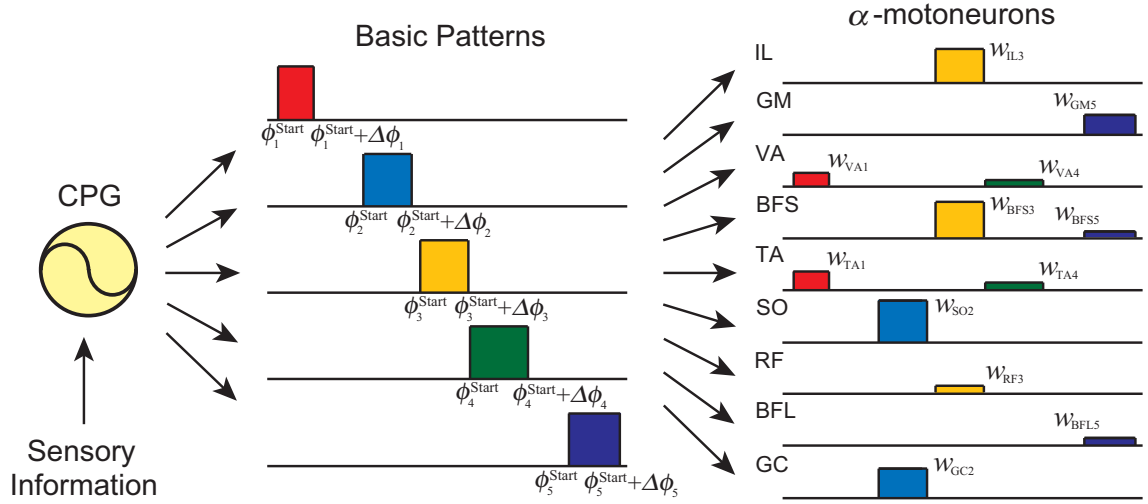
Fig. 3 CPG produces basic patterns delivered to α-motoneurons through neural networks and manages timing of firing based on sensory information

through interneurons. CPGs separately control the locomotor rhythm and pattern of motoneuron activation in the RG and RF networks, respectively.

We modeled the RG and PF networks as a movement controller in our model of the nervous system. For the RG model, we used two simple phase oscillators, each of which produces a basic rhythm and phase information for the corresponding leg, with ϕ_i ($i = left, right$) the oscillator phase for the corresponding leg ($0 \leq \phi_i \leq 2\pi$) and the oscillator phases following the dynamics indicated by

$$\dot{\phi}_{left} = \omega - K_\phi \sin(\phi_{left} - \phi_{right} - \pi)$$
$$\dot{\phi}_{right} = \omega - K_\phi \sin(\phi_{right} - \phi_{left} - \pi) \tag{4}$$

where ω is the basic frequency and K_ϕ the gain parameter. We used $\omega = 2\pi$ rad/s to generate walking motion with a gait cycle of 1.0 s. The second term on the right side indicates a function that maintains interlimb coordination so that the legs move out of phase.

For the PF model, we prepared five rectangular pulses for the basic patterns (Jo and Massaquoi 2007; Jo 2008), whose timing of initiation of bursting and duration depend on oscillator phase ϕ from the RG model, given by

$$CPG_i(\phi) = \begin{cases} 1 \ \phi_i^{Start} \leq \phi < \phi_i^{Start} + \Delta\phi_i \\ 0 \ \text{otherwise} \end{cases} \quad i = 1, \dots, 5 \tag{5}$$

where $CPG_i(\phi)$ ($i = 1, \dots, 5$) is the rectangular pulse, ϕ_i^{Start} the phase value when the rectangular pulse start to burst, and $\Delta\phi_i$ the duration of the rectangular pulse (Fig. 3). These five patterns are

delivered to the α-motoneurons, and output Mov_m from the movement controller is given by

$$Mov_m = \sum_{i=1}^{5} w_{mi} CPG_i(\phi) \tag{6}$$

where w_{mi} is the weighting coefficient for delivery of the five basic patterns to α-motoneurons ($w_{mi} \geq 0$).

To complete this movement controller, we must determine the parameters K_ϕ, ϕ_i^{Start}, $\Delta\phi_i$, and w_{mi}, the total number of which is 56 (=1+5+5+45).

2.3.2 Phase resetting

As noted above, physiological findings suggest that the CPGs manage the timing of firing of the basic patterns based on kinematic events (Ivanenko et al. 2006). In addition, the RG model in the CPGs modulates its basic rhythm by producing phase shifts and rhythm resetting based on sensory information (phase resetting) (Lafreniere-Roula and McCrea 2005; Rybak et al. 2006a).

To model these findings, we reset oscillator phase ϕ based on the kinematic events, in particular foot-contact events (foot contact and foot off), since cutaneous afferents strongly contribute to the observed phase shift and rhythm resetting behaviors (Duysens 1977a; Schomburg et al. 1998). This phase resetting results in the phase shift and rhythm resetting (Aoi et al. 2008; Yamasaki et al. 2003a; Yamasaki et al. 2003b; Nomura et al. 2009). To incorporate phase resetting, we modified oscillator phase dynamics (4) by

$$\dot{\phi}_{left} = \omega - K_\phi \sin(\phi_{left} - \phi_{right} - \pi) - (\phi_{left} - \phi^{Off})\delta(t - t_{left}^{Off} - \tau^{Tactile})$$
$$-(\phi_{left} - \phi^{Contact})\delta(t - t_{left}^{Contact} - \tau^{Tactile})$$
$$\dot{\phi}_{right} = \omega - K_\phi \sin(\phi_{right} - \phi_{left} - \pi) - (\phi_{right} - \phi^{Off})\delta(t - t_{right}^{Off} - \tau^{Tactile})$$
$$-(\phi_{right} - \phi^{Contact})\delta(t - t_{right}^{Contact} - \tau^{Tactile}) \tag{7}$$

where $\delta(\cdot)$ is Dirac's delta function, t_i^{Off} ($i = left, right$) is the time when the foot of the corresponding leg leaves the ground, $t_i^{Contact}$ ($i = left, right$) is the time when the foot lands on the ground, ϕ^{Off} is the phase value to be reset when the foot leaves the ground, and $\phi^{Contact}$ is the phase value to be reset when the foot touches the ground. The third and fourth terms of the right sides constitute the phase resetting, which will reset the oscillator phase ϕ to ϕ^{Off} when the foot leaves the ground and to $\phi^{Contact}$ when the foot touches the ground in order to modulate the timing of firing of the basic patterns and the locomotor rhythm based on sensory information. With resetting of the oscillator phase in the RG model based on foot-contact information, the feedforward signals in the movement control change abruptly between the swing and stance phases. This phase resetting depends on the
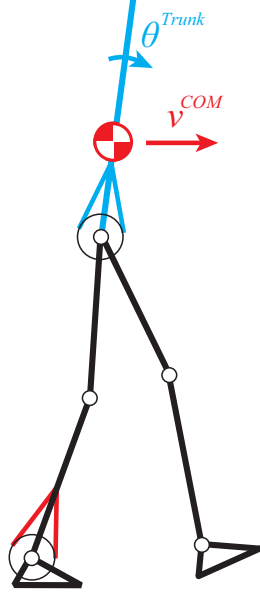
Fig. 4 Posture control based on trunk pitch and horizontal COM velocity

tactile sensor on the foot and the delay in the spinal cord receiving the sensory signal. We set the transmission delay $\tau^{Tactile}$ at 50 ms.

To complete this phase resetting, we must determine the parameters ϕ^{Off} and $\phi^{Contact}$, the total number of which is 2.

2.3.3 Posture control

The brainstem and cerebellum manage posture control based on somatosensory information. In locomotor behavior, it is crucial to maintain a vertical trunk pitch and move the center of mass (COM) forward at the desired velocity (Fig. 4). For simplicity, we focused on these two factors for posture control.

For postural control of trunk pitch, we used simple PD feedback control by muscles IL and GM of the standing leg,

$$Tru_m = \begin{cases} -K_m^{Trunk}(\theta^{Trunk} - \hat{\theta}^{Trunk}) - D_m^{Trunk}\dot{\theta}^{Trunk} & \text{when } GRF > 0 \\ 0 & \text{otherwise} \end{cases} \tag{8}$$

where θ^{Trunk} and $\dot{\theta}^{Trunk}$ are the trunk pitch angle and angular rate, $\hat{\theta}^{Trunk}$ is the reference angle, K_m^{Trunk} and D_m^{Trunk} are the gain parameters ($K_m^{Trunk} = D_m^{Trunk} = 0$ when $m \neq$ IL or GM), and GRF is the vertical ground reaction force. This control aims at simple regulation of the balance of trunk pitch by antagonistic uniarticular muscles in the hip of the standing leg.

For postural control of COM velocity, we used simple feedback control by muscles TA and SO of the standing leg,

$$COM_m = \begin{cases} -K_m^{\text{COM}}(v^{\text{COM}} - \hat{v}^{\text{COM}}) \text{ when } GRF > 0 \\ 0 \hspace{4cm} \text{otherwise} \end{cases} \tag{9}$$

where v^{COM} is the COM velocity, $\hat{v}^{\text{COM}}$ is its desired value, and K_m^{COM} is the gain parameter ($K_m^{\text{COM}} = 0$ when $m \neq$ TA or SO). This control is designed to push the ground when velocity is low and suppress the pushing force when velocity is high simply by means of the uniarticular antagonistic muscles in the ankle of the standing leg.

The command signal from the posture controller is obtained as the summation of these two elements. Since this posture control is managed at the brainstem and cerebellar levels, the command signals are delayed (Fig. 2) and output Pos_m from this posture controller is given by

$$Pos_m(t) = Tru_m(t - \tau^{Somato} - \tau^{Descend}) + COM_m(t - \tau^{Somato} - \tau^{Descend}) \tag{10}$$

where τ^{Somato} and $\tau^{Descend}$ are the delays in receiving transmission of somatosensory information at the brainstem and cerebellar levels and sending the command signal to the spinal cord level, respectively. We assumed $\tau^{Somato} + \tau^{Descend} = 80$ ms.

To make this posture controller function, we must determine the parameters K_m^{Trunk}, D_m^{Trunk}, $\hat{\theta}^{Trunk}$, K_m^{COM}, and $\hat{v}^{\text{COM}}$, the total number of which is 8 (=2+2+1+2+1).

2.4 Determination of parameters in nervous system model

Our model of the nervous system has 66 (=56+2+8) parameters. In this paper, we determined them using the following two-step approach.

In the first step, we used two-dimensional position data for markers attached to the hip, ankle, toe, and heel during human walking in Winter (2004), the gait cycle of which was 1.0 s. We calculated joint kinematics by adapting the position data to our skeletal model, and achieved the desired length profile of each muscle for one gait cycle. We set muscle activation a_m by PD feedback control regarding muscle length to follow the desired length instead of (2), and performed numerical simulation of bipedal locomotion (see details in Aoi et al. (2008)). We performed PCA for the resultant muscle activations to determine parameters ϕ_i^{Start}, $\Delta\phi_i$, and w_{mi} for the basic patterns of movement control and determined parameters $\hat{\theta}^{Trunk}$ and $\hat{v}^{\text{COM}}$ for posture control from the resultant walking behavior.

In the next step, we incorporated the movement and posture controls and phase resetting. We determined muscle activation a_m as the summation of the PD feedback control used in the first step and the command signals from the movement and posture controllers through the low-pass filter

(2). In this step, we determined and modulated parameters w_{mi} for the movement control and gain parameters K_{IL}^{Trunk}, K_{GM}^{Trunk}, D_{IL}^{Trunk}, D_{GM}^{Trunk}, $K_{\text{TA}}^{\text{COM}}$, and $K_{\text{SO}}^{\text{COM}}$ for posture control by trial and error, while decreasing the gain parameters in PD feedback control until the gain parameters in PD feedback control vanished and muscle activations were determined by the movement and posture controls alone. For phase resetting, we determined parameters ϕ^{Off} and $\phi^{Contact}$ so that the phase values just before resetting by delayed tactile sensory information are identical to these parameters during steady walking, specifically, $\phi_{left}(t_{left}^{Off} + \tau^{Tactile}) = \phi^{Off}$, $\phi_{left}(t_{right}^{Off} + \tau^{Tactile}) = \phi^{Off}$, $\phi_{left}(t_{left}^{Contact} + \tau^{Tactile}) = \phi^{Contact}$, and $\phi_{left}(t_{right}^{Contact} + \tau^{Tactile}) = \phi^{Contact}$, which results in the same steady walking both with and without phase resetting.

3 Results

3.1 Generation of normal locomotion

We performed numerical simulation based on our neuromusculoskeletal system model and established steady walking behavior. Figure 5 shows the simulation results. **A** compares the joint angles with the measured kinematic data in Winter (2004), where HC and TO indicate heel contact and toe off, respectively, in the results of simulation. Note that the measured data and the simulation results are shown by aligning the timing of heel contact. During this locomotor behavior, the knee joint reaches the limit angle of the extension (-0.1 rad). **B** compares the vertical and horizontal ground reaction forces with the measured data in Winter (2004). Although the stance phase duration is relatively short, the vertical reaction force has a double-peaked shape and the horizontal reaction force achieves breaking and propulsive forces at the beginning and end of the stance phase, similar to the measured data. **C** shows trunk pitch, which remained nearly vertical during walking. **D** displays the COM velocity, which is 1.4 m/s. **E** illustrates simulated walking behavior with a stick diagram, with a display interval of 0.1 s. **F** shows comparisons of the patterns of activation of the nine muscles with the measured EMG data in Inman (1953) (filled gray areas). This comparison indicates that the numerical simulation successfully yielded results similar to human bipedal locomotion despite the limitations associated with the use of simple rectangular pulses for movement control. The parameters determined for the model of the nervous system are presented in Appendix A.
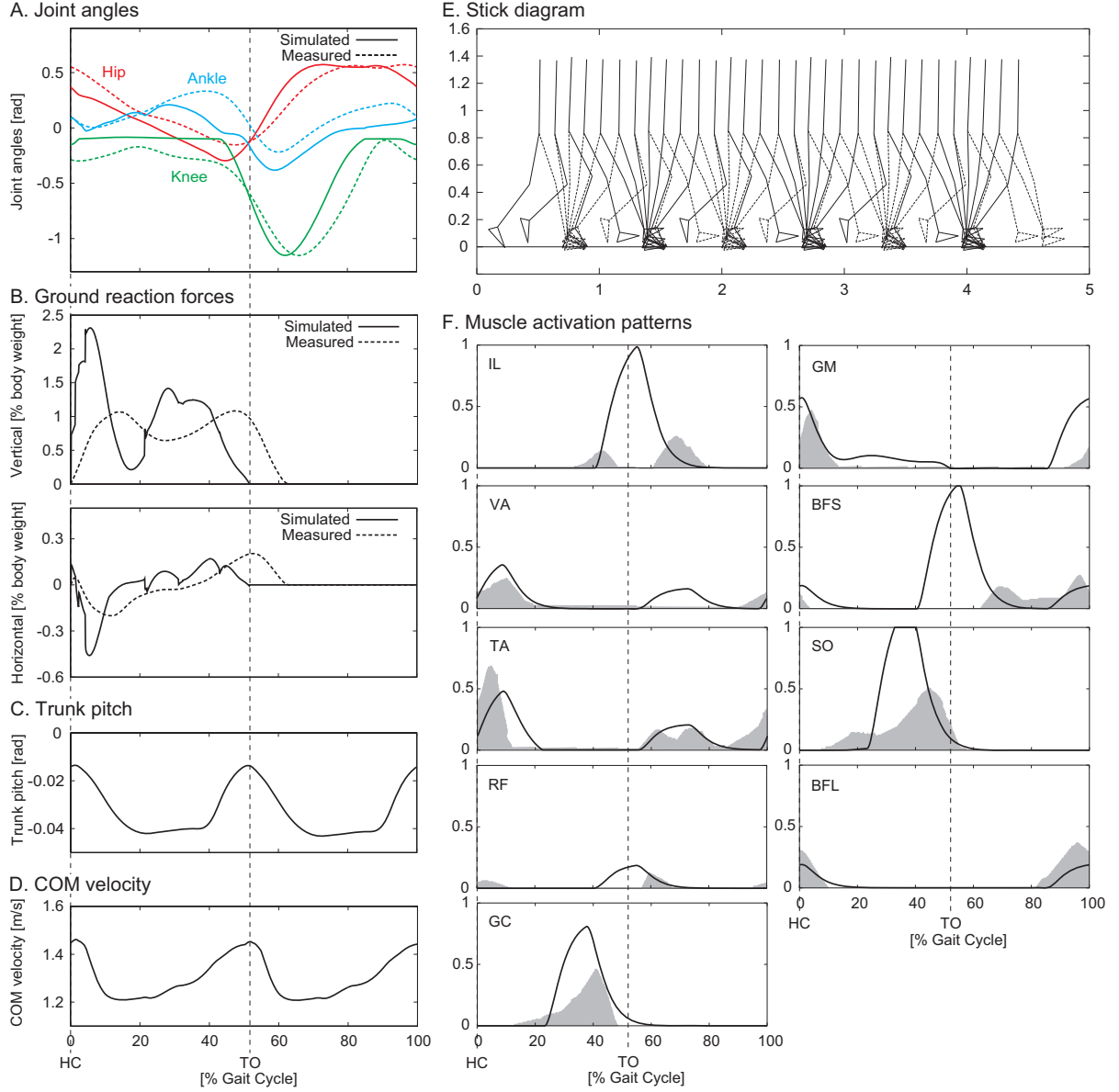
Fig. 5 Results of simulation of normal locomotion. **A**: joint angles, **B**: ground reaction forces, **C**: trunk pitch, **D**: COM velocity, **E**: stick diagram, and **F**: muscle activation patterns. Measured data for joint angles and ground reaction forces are from Winter (2004), and patterns of muscle activation are compared with measured EMG data in Inman (1953) (filled gray areas). HC and TO indicate heel contact and toe off in simulation results.

3.2 Contribution of posture control

The patterns of muscle activation are produced by the command signals from the movement and posture controls. To examine the contributions of posture control during steady walking, we calculated

$$
\frac{\int_{t}^{t+Cycle} |Pos_m(t)| dt}{\int_{t}^{t+Cycle} \{|Mov_m(t)| + |Pos_m(t)|\} dt}
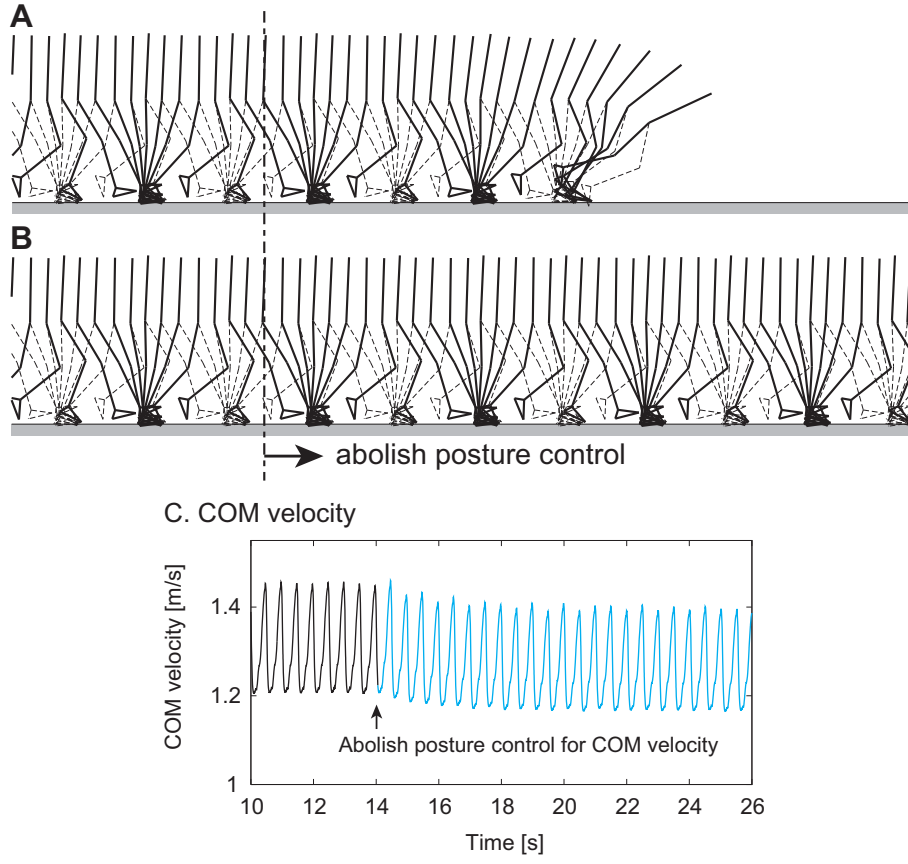\tag{11}
$$

Fig. 6 Simulated walking behavior with abolition of posture control. **A** shows abolition of posture control for trunk pitch. **B** shows abolition of posture control for COM velocity. **C** shows the COM velocity profile with abolition of posture control for COM velocity.

for muscles IL, GM, TA, and SO from Fig. 5, where $Cycle$ is one gait cycle duration ($= 1.0$ s), and found that they were 4, 23, 3, and 4 %, respectively. Although these contributions appear relatively small, they are important in generating walking. When we eliminated posture control from trunk pitch, the walking model could not regulate balance and falling occurred (Fig. 6**A**). Abolition of posture control for COM velocity decreased walking speed, and the resultant COM velocity fluctuated slightly, since adequate propulsive forces could not be obtained (Figs. 6**B** and **C**).

3.3 Contribution of phase resetting

In this section, we thoroughly investigate the roles of phase resetting in achieving adaptive walking against perturbing forces and variations in the environment.
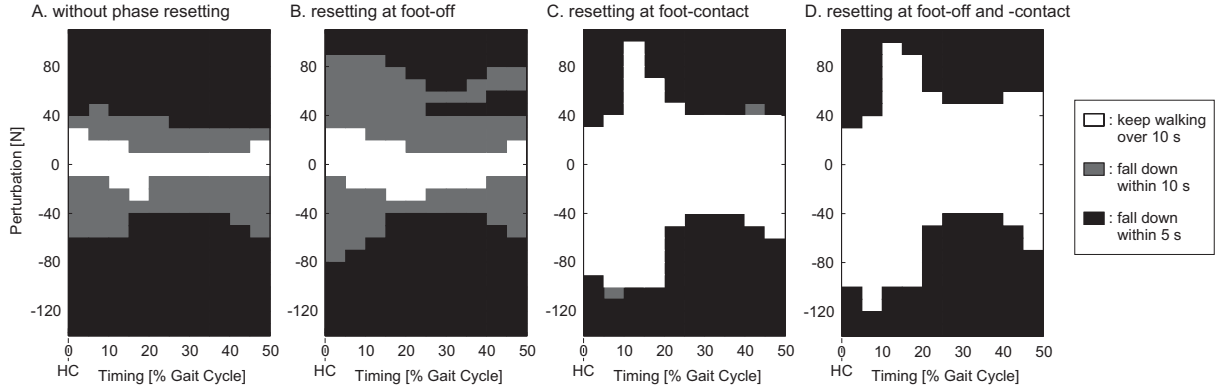
Fig. 7 Tolerance of perturbing forces. **A** shows results without use of phase resetting, **B** the use of phase resetting only at foot off, **C** the use of phase resetting only at foot contact, and **D** the use of phase resetting at both foot off and foot contact.

3.3.1 Tolerance of perturbing forces

First, we examined adaptability to perturbing forces. Since our model employed a phase resetting mechanism based on foot-contact information, we compared four cases: without use of phase resetting, use of phase resetting only at foot off, use of phase resetting only at foot contact, and use of phase resetting at both foot off and foot contact. Specifically, after the walking model achieved steady walking, we added a perturbing force for 0.1 s to the center of mass of HAT in the horizontal direction (forward or backward), and used various magnitudes and timings of the perturbation to thoroughly investigate the robustness of responses.

Figure 7 shows the results of simulation, where white boxes indicate that the walking model continued walking over 10 s after being disturbed, gray boxes indicate that it fell down within 10 s after being disturbed, and black boxes indicate that it fell down within 5 s after being disturbed. When we did not incorporate phase resetting, the model easily fell down. It kept walking longer with use of phase resetting, indicating that phase resetting increased the robustness of responses. The number of white boxes suggests that phase resetting at foot contact contributes more strongly to responses to perturbing forces than phase resetting at foot off. Use of phase resetting at both foot off and foot contact yielded the greatest degree of robustness among these four cases.

Figure 8 shows the trunk pitch and COM velocity profiles demonstrating the contribution of phase resetting to the response of the perturbation; without use of phase resetting (**A**) and with use of phase resetting at both foot off and foot contact (**B**). In Fig. 8**A**, red lines show a perturbation of 2 Ns at 0 % of gait cycle after foot contact, while blue lines show a perturbation of −2 Ns at 15 % of gait cycle after foot contact. In Fig. 8**B**, red lines show a perturbation of 7 Ns at 15 % of gait cycle after foot contact, while blue lines show a perturbation of −7 Ns at 10 % of gait cycle after foot contact. When

A. without phase resetting
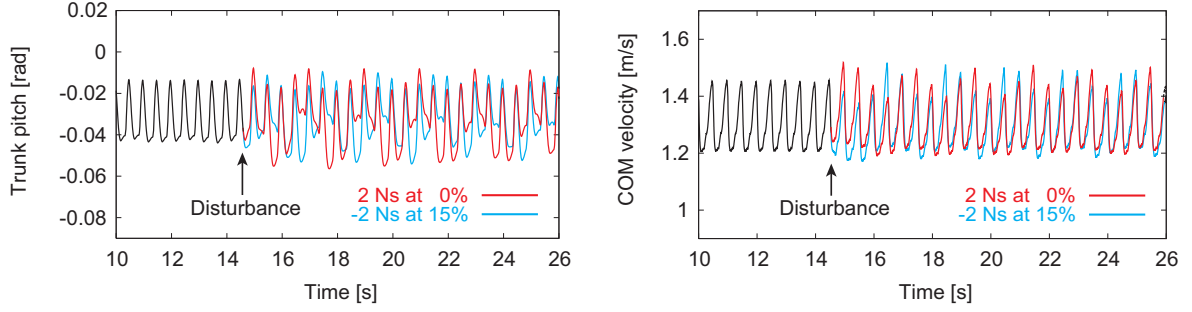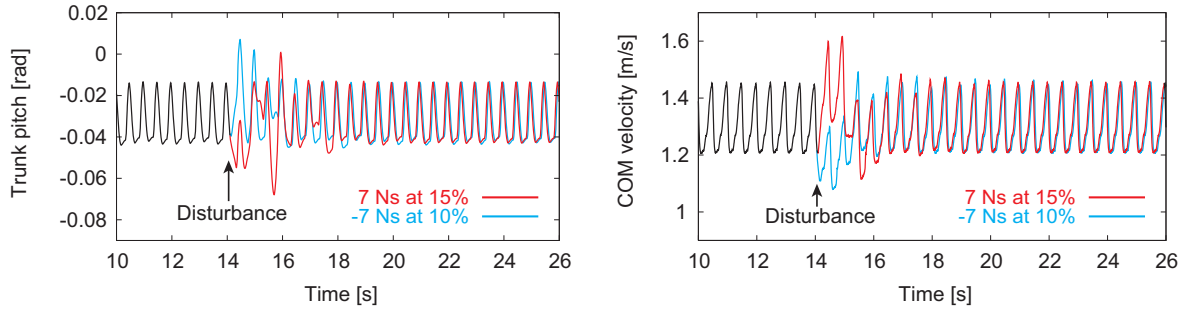

B. with phase resetting

Fig. 8 Response of perturbation for trunk pitch and COM velocity. **A** shows results without use of phase resetting and **B** the use of phase resetting at both foot off and foot contact.

phase resetting was not used, the trunk pitch and COM velocity still fluctuated 10 s after they were disturbed. In contrast, with use of phase resetting, they recovered quickly.

3.3.2 Roles of interlimb coordination

To investigate the roles of interlimb coordination, we examined tolerance of perturbing forces in the same fashion as in the preceding section. Specifically, we performed similar simulations to those in the preceding section using various values of gain parameter K_ϕ in (7) and phase resetting at both foot-off and foot-contact events, depicted results as in Fig. 7, and counted the numbers of white boxes indicating that the walking model continued walking over 10 s after being disturbed as successful trials.

Figure 9 shows the results of simulation. The gain parameter $K_\phi = 1.7$ used in our model exhibited the most robustness against perturbing forces; smaller and larger gain parameters decreased robustness. When a value smaller than 0.8 or larger than 3.4 is used for the gain parameter, robustness is lower than without use of phase resetting, suggesting the importance of adequate control of interlimb coordination during walking.
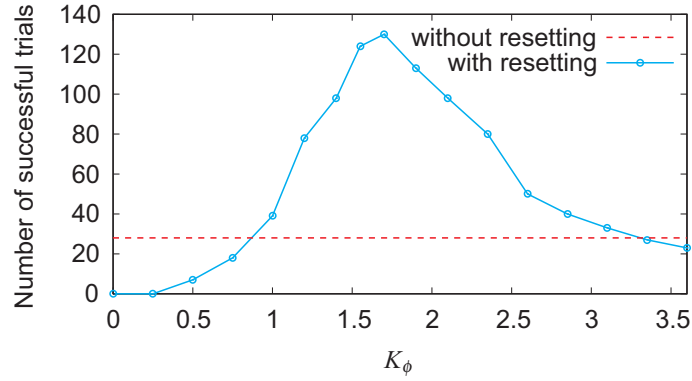
Fig. 9 Tolerance of perturbing forces in gain parameter K_ϕ

3.3.3 Adaptation to sudden increase in trunk mass

To examine robustness against sudden increase in trunk mass, we compared two cases, without use of phase resetting and use of phase resetting at both foot off and foot contact. The walking model could maintain walking with an increase of up to 2.8 kg in trunk mass without falling over when we did not use phase resetting. In contrast, it could continue walking with an increase of up to 4.2 kg in trunk mass with the use of phase resetting.

Figure 10 demonstrates simulated walking behavior when trunk mass was suddenly increased by 3.2 kg. When we did not use phase resetting, walking speed decreased and the figure stumbled (Figs. 10**A** and **C**). However, with the use of phase resetting, it continued walking without falling (Fig. 10**B**). Since the initial foot-contact was earlier due to the sudden increase in trunk mass, the walking rhythm was interrupted earlier by phase resetting (Fig. 10**D**). After several steps to adapt to the sudden increase in trunk mass, walking speed decreased (Fig. 10**C**) and foot-contact events were delayed, with increase in the amount of phase resetting (Fig. 10**D**) and in the gait cycle (Fig. 10**E**). This environmental variation changed the hip and ankle joint profiles (Fig. 10**F**), illustrating the kinematic effects of this adaptation.

3.3.4 Adaptation to sudden change in slope angle

To investigate robustness against sudden change in slope angle, we also compared two cases, without the use of phase resetting and with the use of phase resetting at both foot off and foot contact. Without phase resetting, the walking model could climb a slope up to 0.74 deg without falling, but with the use of phase resetting, the model could climb a slope up to 1.20 deg. Without phase resetting, the model could walk down a slope up to −0.45 deg, and with phase resetting, the model could walk down a slope up to −0.74 deg.
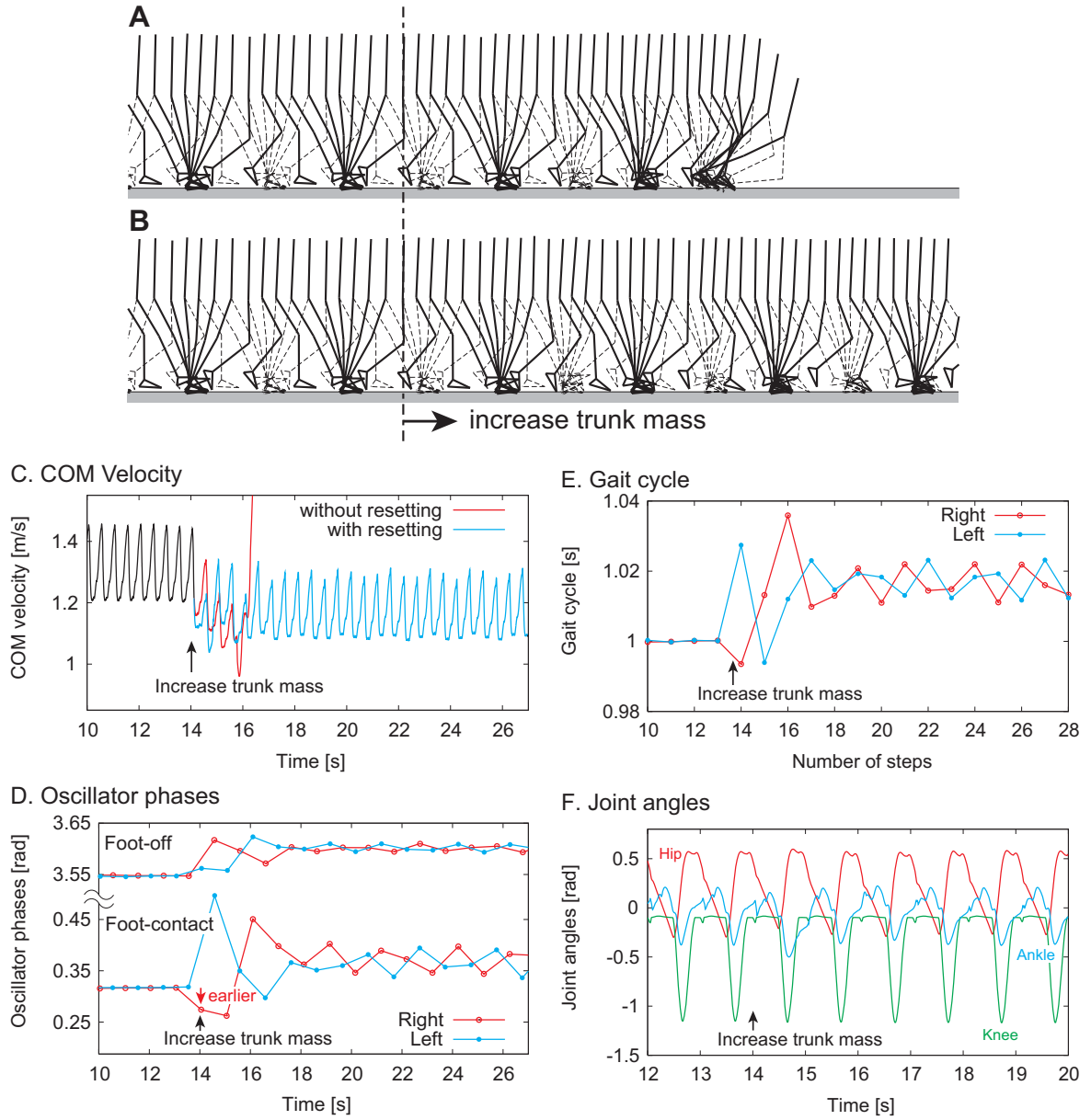
Fig. 10 Simulated walking behavior with sudden increase of 3.2 kg in trunk mass. **A** and **B** show stick diagrams without and with phase resetting, respectively, **C** is the COM velocity profile, **D** shows oscillator phase values just before resetting based on foot-contact events, **E** is gait cycle duration, and **F** shows joint angle profiles.

Figures 11 and 12 illustrate simulated walking behavior with the ground changed from flat to an upslope of 1.15 deg and a downslope of −0.57 deg, respectively. Although the model fell without phase resetting (Figs. 11**A** and 12**A**), it continued walking without falling and established steady walking with incorporation of phase resetting (Figs. 11**B** and 12**B**). In upslope locomotion, the initial foot-contact was earlier due to the sudden increase in slope angle, and the walking rhythm was interrupted by phase resetting (Fig. 11**D**). In contrast, in downslope locomotion, the initial foot-contact was delayed
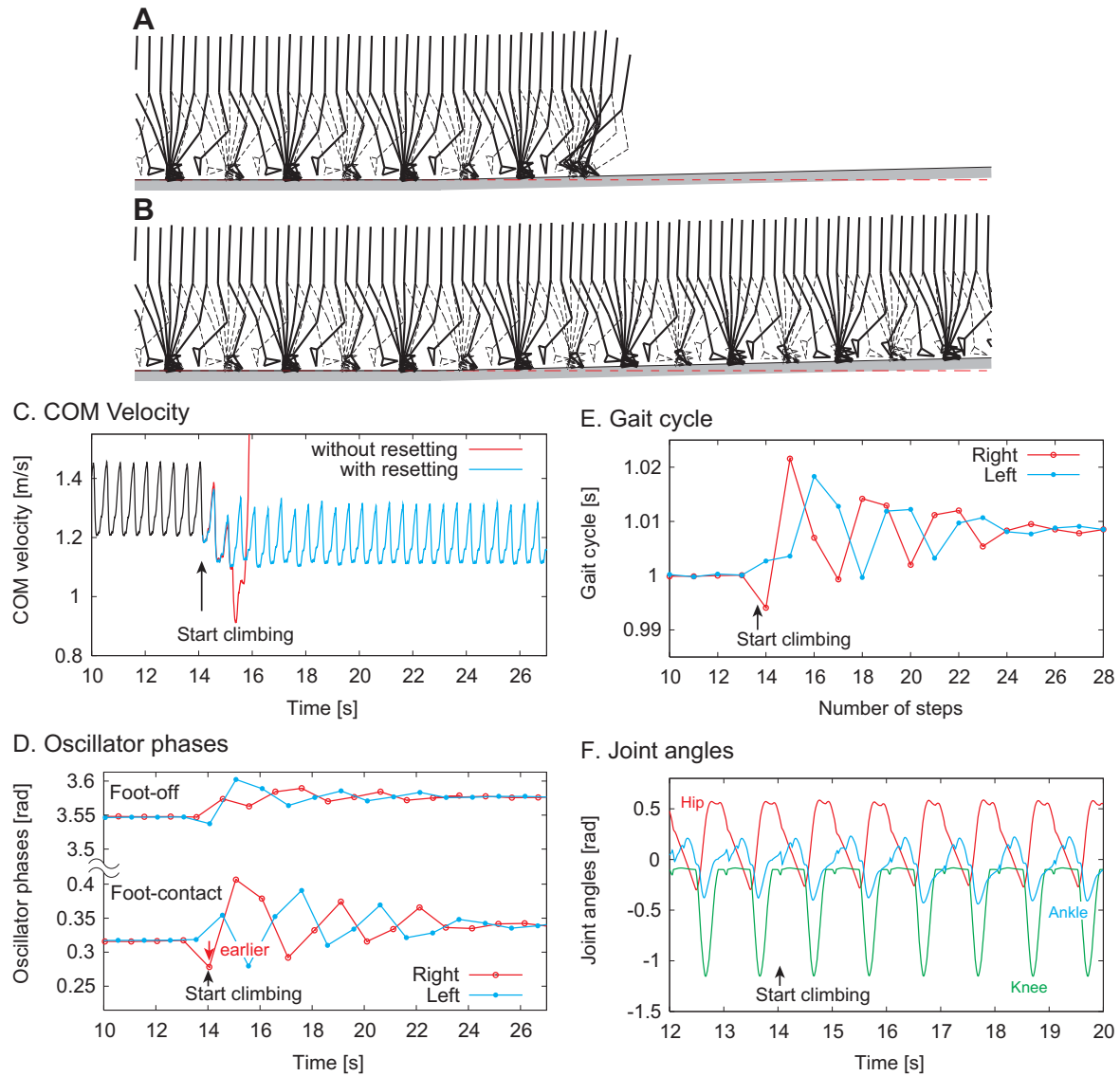
Fig. 11 Simulated walking behavior with change in ground from flat to upslope. **A** and **B** show stick diagrams without and with phase resetting, respectively, **C** is the COM velocity profile, **D** shows oscillator phase values just before resetting based on foot-contact events, **E** is gait cycle duration, and **F** shows joint angle profiles.

due to the sudden decrease in slope angle, and the walking rhythm was prolonged by phase resetting (Fig. 12**D**). Upon final adaptation to the upslope, walking speed was decreased (Fig. 11**C**) and the foot-contact events were delayed, resulting in an increase in the amount of phase resetting (Fig. 11**D**) and in the gait cycle (Fig. 11**E**). On the other hand, in adapting to the downslope, walking speed increased (Fig. 12**C**) and foot-contact events occurred earlier (Fig. 12**D**), resulting in a decrease in the gait cycle (Fig. 12**E**). These environmental variations changed the hip and ankle joint profiles (Figs. 11**F** and 12**F**), and the feet came into contact with the ground not from the heel but with the flat sole on the upslope, illustrating the kinematic effects of adaptation.
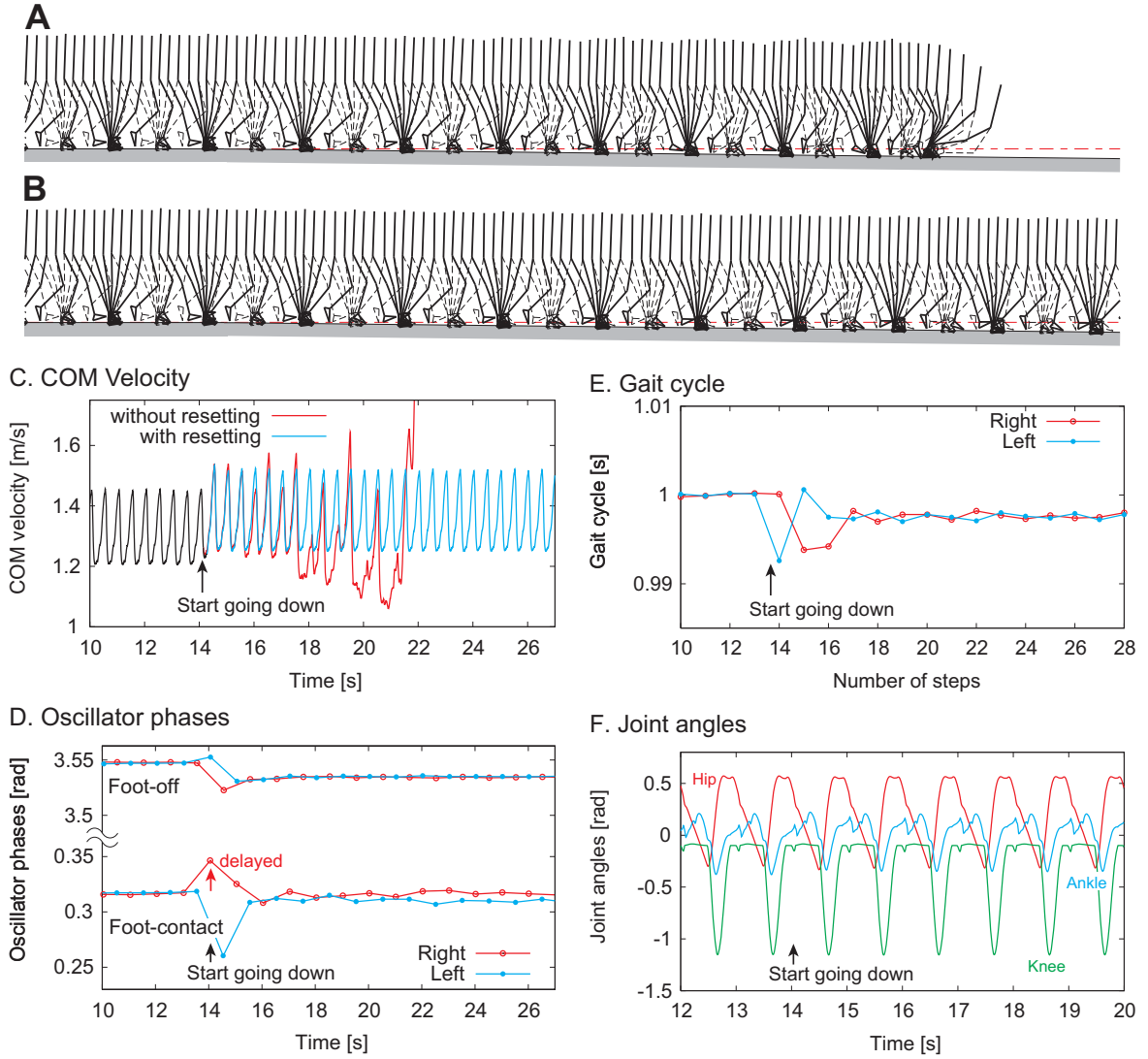
Fig. 12 Simulated walking behavior when ground changes from flat to downslope. **A** and **B** show stick diagrams without and with phase resetting, respectively, **C** is the COM velocity profile, **D** shows oscillator phase values just before resetting based on foot-contact events, **E** is gait cycle duration, and **F** shows joint angle profiles.

These results suggest that phase resetting improves adaptability to environmental variations.

4 Discussion

The roles of phase resetting during human bipedal walking have previously been investigated assuming that locomotion is generated based on prescribed kinematics and feedback control (Aoi *et al.* 2008; Yamasaki *et al.* 2003a; Yamasaki *et al.* 2003b; Nomura *et al.* 2009). However, this study for the first time incorporated the feedforward nature of neuro-control mechanisms and its hypothetical phase resetting in a simulation model to generate bipedal walking. As a result of our effort to construct a more

physiologically-based model of control of animal locomotion, we successfully generated robust, adaptive human walking despite the inclusion of substantial time delays attributable to neural transmission. Furthermore, gait kinematics could be autonomously altered to cope with external perturbations and environmental changes, since they were not predetermined as in our previous study based on feedback control (Aoi *et al.* 2008).

The present study demonstrated that phase resetting actually contributes to the generation of robust bipedal walking. The spatiotemporal patterns of command signals determine locomotor behavior, and phase resetting results in temporal modulation of this behavior based on foot-contact events. Even if the timing of events is disturbed due to external perturbations and environmental variations, phase resetting allows command signals to be produced based on such events. Early foot-contact events induce early production of command signals, which interrupts the locomotor rhythm, as demonstrated in the cases of sudden increase in trunk mass (Fig. 10**D**) and sudden change to upslope (Fig. 11**D**). In contrast, delayed foot-contact events result in delayed production of command signals, which prolongs the locomotor rhythm, as demonstrated in the case of sudden change to downslope (Fig. 12**D**). Phase resetting creates various phase profiles and walking rhythms that depend on the situation, and thus modulates gait kinematics and improves the adaptability of locomotor behavior. More specifically, phase resetting increases the basin of attraction (Fig. 7) and the convergence rate to undisturbed locomotor behavior (Fig. 8) as examined using perturbing forces, and improves the robustness to various environmental changes (Figs. 10, 11, and 12).

Foot-contact events occur intermittently during locomotion and phase resetting modulates the oscillator phase of the corresponding leg in the RG model, which influences the phase difference between the oscillators. Since the phase of the oscillators determines the command signals of the corresponding leg in the PF model, the relationship between the oscillators contributes to the interlimb coordination. This relationship is controlled by the gain parameter K_ϕ in the oscillator phase dynamics (7). A small value for the gain parameter can not maintain an adequate phase relationship, while a large value induces abrupt changes. To create adaptive locomotor behavior, as well as phase resetting, adequate control of interlimb coordination is also crucial (Fig. 9).

The functional roles of sensory regulation similar to phase resetting have been investigated in cat locomotion. Cats are known to use two types of sensory information to change phase from stance to swing: force-sensitive afferents (Duysens and Pearson 1980; Whelan *et al.* 1995) and position-sensitive afferents (Grillner and Rossignol 1978; Hiebert *et al.* 1996). Ekeberg and Pearson (2005) performed numerical simulations with a musculoskeletal model of the hind limbs to investigate the roles of these types of sensory information, and their findings suggested that the phase transition induced by force information makes a larger contribution than position information to the generation of adaptive lo-

comotor behavior. Yakovenko *et al.* (2004) modeled feedforward command signals for the swing and stance phases delivered to motoneurons from measured EMG data and devised a feedback controller based on local muscle information by modeling of stretch reflexes. They switched the phases of feedforward commands based on joint configuration and tactile sensory information that induced phase resetting. Their modeling of control mechanisms resembles ours, and their results of simulation, suggesting that phase and rhythm modulations play important roles in establishing adaptive walking, appear to support our model of regulation of phase resetting in human bipedal walking.

To construct a biologically accurate nervous system model, it is necessary to include signal transmission delay. Since the command signals are produced by integrating input from higher centers and afferent feedback, such delays strongly influence the locomotor behavior. In our nervous system model, the posture control creates command signals in a feedback fashion based on delayed somatosensory information and large values can not be used for the gain parameters due to the transmission delay. Therefore, although posture control is important for generating locomotor behavior (Fig. 6), it has limitations and can cope with only small and slow disturbances. For large and fast disturbances, it is necessary to incorporate adequate modeling of reflex mechanisms.

In this paper, we confined the musculoskeletal model to two dimensions and modeled the nervous system in simple fashion. We used five rectangular pulses for movement control, which limited the shapes of the command signals. For posture control, we employed control mechanisms based only on trunk pitch and COM velocity using uniarticular muscles at the hips and ankles. Although the results of such simple modeling differed to some extent from actual human bipedal locomotion, e.g., simulated double stance duration was short (Fig. 5**B**), our simulation results were similar to the features of human walking both kinematically and kinetically, and clearly demonstrated the functional roles of sensory regulation in phase resetting. However, phase resetting could not fully explain the adaptability observed in human walking and we can not deny the possibility that the contribution of phase resetting is relatively small since the present study relies a lot on the model parameters tuned to generate the walking without phase resetting. To create a more sophisticated and plausible model, more adequate mechanisms, such as reflex mechanisms, need to be incorporated in future studies.

A Parameters in nervous system model

A.1 Parameters for movement controller

Based on the PCA for patterns of muscle activation using PD feedback control with measured kinematic data, we determined the parameters for the five basic patterns ($CPG_{1\cdots5}$) as follows: $\phi_1^{Start} = 6.10$ rad, $\phi_2^{Start} = 1.45$ rad, $\phi_3^{Start} = 2.53$ rad, $\phi_4^{Start} = 3.48$ rad, $\phi_5^{Start} = 5.35$ rad, $\Delta\phi_1 = 0.70$ rad, $\Delta\phi_2 = 0.90$ rad,

$\Delta\phi_3 = 0.90$ rad, $\Delta\phi_4 = 1.07$ rad, and $\Delta\phi_5 = 0.96$ rad, where we set $\phi = 0$ rad at heel contact. Since these basic patterns contribute to the specific responses of α-motoneurons, we set the weighting coefficients for the basic patterns that deliver inputs to the α-motoneurons that have small contribution 0 as follows: $w_{m1} = 0$ ($m \neq$ VA or TA), $w_{m2} = 0$ ($m \neq$ SO or GC), $w_{m3} = 0$ ($m \neq$ IL, BFS, or RF), $w_{m4} = 0$ ($m \neq$ VA or TA), and $w_{m5} = 0$ ($m \neq$ GM, BFS, or BFL). The other weighting coefficients were determined through modulation of the second step of parameter determination as follows: $w_{\mathrm{VA}1} = 0.42$, $w_{\mathrm{TA}1} = 0.56$, $w_{\mathrm{SO}2} = 1.26$, $w_{\mathrm{GC}2} = 0.87$, $w_{\mathrm{IL}3} = 1.04$, $w_{\mathrm{BFS}3} = 1.09$, $w_{\mathrm{RF}3} = 0.20$, $w_{\mathrm{VA}4} = 0.17$, $w_{\mathrm{TA}4} = 0.21$, $w_{\mathrm{GM}5} = 0.61$, $w_{\mathrm{BFS}5} = 0.20$, and $w_{\mathrm{BFL}5} = 0.20$. Gain parameter K_ϕ, which controls interlimb coordination, was determined to obtain a high degree of robustness against perturbing forces (Sec. 3.3.2) as follows: $K_\phi = 4.0$ for phase resetting only at foot off, $K_\phi = 2.0$ for phase resetting only at foot contact, and $K_\phi = 1.7$ for phase resetting at both foot off and foot contact.

A.2 Parameters for phase resetting

We set $\phi^{Off} = 3.55$ rad and $\phi^{Contact} = 0.31$ rad, so that the phase values just before resetting based on delayed tactile sensory information are identical to these parameters during steady walking, that is, $\phi_{left}(t_{left}^{Off} + \tau^{Tactile}) = \phi^{Off}$, $\phi_{left}(t_{right}^{Off} + \tau^{Tactile}) = \phi^{Off}$, $\phi_{left}(t_{left}^{Contact} + \tau^{Tactile}) = \phi^{Contact}$, and $\phi_{left}(t_{right}^{Contact} + \tau^{Tactile}) = \phi^{Contact}$. Therefore, the steady walking with phase resetting is almost the same as the steady walking without phase resetting, which allows us to clearly investigate the difference only of the response to external perturbations and environmental changes.

A.3 Parameters for posture controller

From the results of simulation using PD feedback control with measured kinematic data, we obtained $\hat{\theta}^{Trunk} = -0.012$ rad and $\hat{v}^{\mathrm{COM}} = 1.4$ m/s. The gain parameters were determined through modulation of the second step of parameter determination as follows: $K_{\mathrm{IL}}^{Trunk} = -1.0$, $K_{\mathrm{GM}}^{Trunk} = 2.0$, $D_{\mathrm{IL}}^{Trunk} = -0.2$, $D_{\mathrm{GM}}^{Trunk} = 0.4$, $K_{\mathrm{TA}}^{\mathrm{COM}} = -0.4$, and $K_{\mathrm{SO}}^{\mathrm{COM}} = 0.12$.

References

Aoi *et al.* 2008. Aoi, S., Ogihara, N., Sugimoto, Y., and Tsuchiya, K. (2008) *Simulating adaptive human bipedal locomotion based on phase resetting using foot-contact information*, Adv. Robot., 22:1697–1713.

Burke *et al.* 2001. Burke, R.E., Degtyarenko, A.M., and Simon, E.S. (2001) *Patterns of locomotor drive to motoneurons and last-order interneurons: Clues to the structure of the CPG*, J. Neurophysiol., 86:447–462.

Conway *et al.* 1987. Conway, B.A., Hultborn, H., and Kiehn, O. (1987) *Proprioceptive input resets central locomotor rhythm in the spinal cat*, Exp. Brain Res., 68:643–656.

Danna-dos-Santos *et al.* 2007. Danna-dos-Santos, A., Slomka, K., Zatsiorsky, V.M., and Latash, M.L. (2007) *Muscle modes and synergies during voluntary body sway*, Exp. Brain Res., 179:533–550.

d'Avella and Bizzi 2005. d'Avella, A. and Bizzi, E. (2005) *Shared and specific muscle synergies in natural motor behaviors*, Proc. Natl. Acad. Sci. USA, 102(8):3076–3081.

d'Avella *et al.* 2003. d'Avella, A., Saltiel, P., and Bizzi, E. (2003) *Combinations of muscle synergies in the construction of a natural motor behavior*, Nat. Neurosci., 6:300–308.

Davy and Audu 1987. Davy, D.T. and Audu, M.L. (1987) *A dynamic optimization technique for predicting muscle forces in the swing phase of gait*, J. Biomech., 20(2):187–201.

Drew *et al.* 2008. Drew, T., Kalaska, J., and Krouchev, N. (2008) *Muscle synergies during locomotion in the cat: a model for motor cortex control*, J. Physiol., 586(5):1239–1245.

Duysens and Pearson 1980. Duysens, J. and Pearson, K.G. (1980) *Inhibition of flexor burst generation by loading ankle extensor muscles in walking cats*, Brain Res., 187:321–332.

Duysens 1977a. Duysens, J. (1977) *Fluctuations in sensitivity to rhythm resetting effects during the cat's step cycle*, Brain Res., 133(1):190–195.

Ekeberg and Pearson 2005. Ekeberg, Ö. and Pearson, K. (2005) *Computer simulation of stepping in the hind legs of the cat: An examination of mechanisms regulating the stance-to-swing transition*, J. Neurophysiol., 94:4256–4268.

Frigon and Rossignol 2006. Frigon, A. and Rossignol, S. (2006) *Experiments and models of sensorimotor interactions during locomotion*, Biol. Cybern., 95:607–627.

Fuglevand and Winter 1993. Fuglevand, A.J. and Winter, D.A. (1993) *Models of recruitment and rate coding organization in motor-unit pools*, J. Neurophysiol., 70(6):2470–2488.

Grillner 1975. Grillner, S. (1975) *Locomotion in vertebrates: central mechanisms and reflex interaction*, Physiol. Rev., 55(2):247–304.

Grillner and Rossignol 1978. Grillner, S. and Rossignol, S. (1978) *On the initiation of the swing phase of locomotion in chronic spinal cats*, Brain Res., 146:269–277.

Guertin *et al.* 1995. Guertin, P., Angel, M.J., Perreault, M.-C., and McCrea, D. A. (1995) *Ankle extensor group I afferents excite extensors throughout the hindlimb during fictive locomotion in the cat*, J. Physiol., 487(1):197–209.

Guertin 2009. Guertin, P.A. (2009) *The mammalian central pattern generator for locomotion*, Brain Res. Rev., 62:45–56.

Hiebert *et al.* 1996. Hiebert, G.W., Whelan, P.J., Prochazka, A., and Pearson, K.G. (1996) *Contribution of hindlimb flexor muscle afferents to the timing of phase transitions in the cat step cycle*, J. Neurophysiol., 75:1126–1137.

Hultborn and Nielsen 2007. Hultborn, H. and Nielsen, J.B. (2007) *Spinal control of locomotion – from cat to man*, Acta Physiol., 189:111–121.

Inman 1953. Inman, V.T. (1953) *The pattern of muscular activity in the lower extremity during walking (Technical Report Series II, No. 25)*, Prosthetic Devices Research Project, Institute of Engineering Research, University of California, Berkeley, Calif.

Ivanenko *et al.* 2004. Ivanenko, Y.P., Poppele, R.E., and Lacquaniti, F. (2004) *Five basic muscle activation patterns account for muscle activity during human locomotion*, J. Physiol., 556:267–282.

Ivanenko *et al.* 2006. Ivanenko, Y.P., Poppele, R.E., and Lacquaniti, F. (2006) *Motor control programs and walking*, Neuroscientist, 12(4):339–348.

Ivanenko *et al.* 2005. Ivanenko, Y.P., Cappellini, G., Dominici, N., Poppele, R.E., and Lacquaniti, F. (2005) *Coordination of locomotion with voluntary movements in humans*, J. Neurosci., 25(31):7238–7253.

Ijspeert 2001. Ijspeert, A.J. (2001) *A connectionist central pattern generator for the aquatic and terrestrial gaits of a simulated salamander*, Biol. Cybern., 84:331–348.

Jo and Massaquoi 2007. Jo, S. and Massaquoi, S.G. (2007) *A model of cerebrocerebello-spinomuscular interaction in the sagittal control of human walking*, Biol. Cybern., 96:279–307.

Jo 2008. Jo, S. (2008) *Hypothetical neural control of human bipedal walking with voluntary modulation*, Med. Bio. Eng. Comput., 46:179–193.

Lafreniere-Roula and McCrea 2005. Lafreniere-Roula, M. and McCrea, D.A. (2005) *Deletions of rhythmic motoneuron activity during fictive locomotion and scratch provide clues to the organization of the mammalian central pattern generator*, J. Neurophysiol., 94:1120–1132.

McCrea and Rybak 2008. McCrea, D.A. and Rybak, I.A. (2008) *Organization of mammalian locomotor rhythm and pattern generation*, Brain Res. Rev., 57:134–146.

Minassian *et al.* 2007. Minassian, K., Persy, I., Rattay, F., Pinter, M.M., Kern, H., and Dimitrijevic, M.R. (2007) *Human lumbar cord circuitries can be activated by extrinsic tonic input to generate locomotor-like activity*, Hum. Mov. Sci., 26:275–295.

Nomura *et al.* 2009. Nomura, T., Kawa, K., Suzuki, Y., Nakanishi, M., and Yamasaki, T. (2009) *Dynamic stability and phase resetting during biped gait*, Chaos, 19, 026103.

Ogihara and Yamazaki 2001. Ogihara, N. and Yamazaki, N. (2001) *Generation of human bipedal locomotion by a bio-mimetic neuro-musculo-skeletal model*, Biol. Cybern., 84:1–11.

Orlovsky *et al.* 1999. Orlovsky, G.N., Deliagina, T., and Grillner, S. (1999) Neuronal control of locomotion: from mollusc to man, *Oxford University Press*.

Rybak *et al.* 2006a. Rybak, I.A., Shevtsova, N.A., Lafreniere-Roula, M., and McCrea, D.A. (2006) *Modelling spinal circuitry involved in locomotor pattern generation: insights from deletions during fictive locomotion*, J. Physiol., 577(2):617–639.

Rybak *et al.* 2006b. Rybak, I.A., Stecina, K., Shevtsova, N.A., and McCrea, D.A. (2006) *Modelling spinal circuitry involved in locomotor pattern generation: insights from the effects of afferent stimulation*, J. Physiol., 577(2):641–658.

Schomburg *et al.* 1998. Schomburg, E.D., Petersen, N., Barajon, I., and Hultborn, H. (1998) *Flexor reflex afferents reset the step cycle during fictive locomotion in the cat*, Exp. Brain Res., 122(3):339–350.

Shik and Orlovsky 1976. Shik, M.L. and Orlovsky, G.N. (1976) *Neurophysiology of locomotor automatism*, Phsyiol. Rev., 56(3):465–501.

Taga *et al.* 1991. Taga, G., Yamaguchi, Y., and Shimizu, H. (1991) *Self-organized control of bipedal locomotion by neural oscillators in unpredictable environment*, Biol. Cybern., 65:147–159.

Taga 1995a. Taga, G. (1995) *A model of the neuro-musculo-skeletal system for human locomotion I. Emergence of basic gait*, Biol. Cybern., 73:97–111.

Taga 1995b. Taga, G. (1995) *A model of the neuro-musculo-skeletal system for human locomotion II. - Real-time adaptability under various constraints*, Biol. Cybern., 73:113–121.

Ting and Macpherson 2005. Ting, L.H. and Macpherson, J.M. (2005) *A limited set of muscle synergies for force control during a postural task*, J. Neurophysiol., 93:609–613.

Todorov and Jordan 2002. Todorov, E. and Jordan, M.I. (2002) *Optimal feedback control as a theory of motor coordination*, Nat. Neurosci., 5:1226–1235.

Wadden and Ekeberg 1998. Wadden, T. and Ekeberg, Ö. (1998) *A neuro-mechanical model of legged locomotion: single leg control*, Biol. Cybern., 79:161–173.

Whelan *et al.* 1995. Whelan, P.J., Hiebert, G.W., and Pearson, K.G. (1995) *Stimulation of the group I extensor afferents prolongs the stance phase in walking cats*, Brain Res., 103:20–30.

Winter 2004. Winter, D.A. (2004) Biomechanics and motor control of human movement (3rd edition), *New York: John Wiley & Sons.*

Yakovenko *et al.* 2004. Yakovenko, S., Gritsenko, V., and Prochazka, A. (2004) *Contribution of stretch reflexes to locomotor control: A modeling study*, Biol. Cybern., 90:146–155.

Yamasaki *et al.* 2003a. Yamasaki, T., Nomura, T., and Sato, S. (2003) *Phase reset and dynamic stability during human gait*, BioSystems, 71:221–232.

Yamasaki *et al.* 2003b. Yamasaki, T., Nomura, T., and Sato, S. (2003) *Possible functional roles of phase resetting during walking*, Biol. Cybern., 88:468–496.